THE JOURNAL OF PHYSICAL CHEMISTRY B

ARTICLE

pubs.acs.org/JPCB

Quantum Chemical Analysis of the Unfolding of a Penta-alanyl 3_{10}-Helix Initiated by $HO^{\bullet}$, $HO_2^{\bullet}$ and $O_2^{-\bullet}$

Michael C. Owen,[†,‡,§,∥] Bela Viskolcz,[*,‡,∥] and Imre G. Csizmadia[†,‡,§,∥]

[†]Department of Chemistry, University of Toronto, Toronto, Ontario M5S 3H6, Canada

[‡]Department of Chemical Informatics, Faculty of Education, University of Szeged, Boldogasszony sgt. 6, H-6725 Szeged, Hungary

[§]Global Institute of Computational Molecular and Materials Science, Toronto, Ontario M5S 2K2, Canada

[∥]Drug Discovery Research Center, University of Szeged, Boldogasszony sgt. 6, H-6725 Szeged, Hungary

Supporting Information

ABSTRACT: In order to elucidate the mechanisms of radical-initiated unfolding of a helix, the thermodynamic functions of hydrogen abstraction from the C_α, C_β, and amide nitrogen of Ala^3 in a homopeptapeptide (*N*-Ac-AAAAA-NH_2; A5) by $HO^{\bullet}$, $HO_2^{\bullet}$, and $O_2^{-\bullet}$ were computed using the B3LYP density functional. The thermodynamic functions, standard enthalpy (ΔH°), Gibbs free energy (ΔG°), and entropy (ΔS°), of the reactants and products of these reactions were computed with A5 in the 3_{10}-helical ($A5_{Hel}$) and fully extended ($A5_{Ext}$) conformations at the B3LYP/6-31G(d) and B3LYP/6-311+G(d,p) levels of theory, both in the gas phase and using the C-PCM implicit water model. With quantum chemical calculations, we have shown that H abstraction is the most favorable at the C_α, followed by the C_β, then amide N in a model helix. The secondary structure has a strong influence on the bond dissociation energy of the H−C_α, but a negligible effect on the dissociation energy of the H−CH_2 and H−N bonds. The $HO^{\bullet}$ radical is the strongest hydrogen abstractor, followed by $HO_2^{\bullet}$ and finally $O_2^{-\bullet}$. More importantly, secondary structure elements, such as H-bonds in the 3_{10}-helix, protect the peptide from radical attack by hindering the potential electron delocalization at the C_α when the peptide is in the extended conformation. We also show that he unfolding of the A5 peptide radicals have a significantly higher propensity to unfold than the closed shell A5 peptide and confirm that only the $HO^{\bullet}$ can initiate the unfolding of $A5_{Hel}$ and the formation of $A5_{Ext}^{\bullet}$. By comparing the structures, energies, and thermodynamic functions of A5 and its radical derivatives, we have shown how free radicals can initiate the unfolding of helical structures to β-sheets in the cellular condition known as oxidative stress.

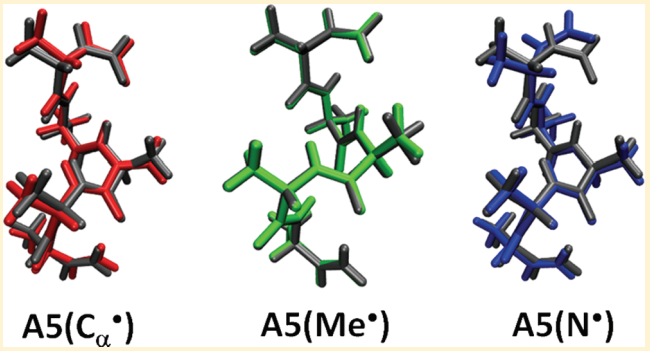

1. INTRODUCTION

O_2 has evolved to be the terminal electron acceptor in the oxidation of carbon fuels to generate adenosine triphosphate (ATP) by oxidative phosphorylation. However, the physiological role of O_2 is not limited to energy metabolism. The metabolism of sterols, indoles, alkaloids, antibiotics, and some detoxifying pathways are also O_2-dependent.[1] The metabolic analysis of 70 genomes suggested that O_2 is directly or indirectly associated with over a thousand metabolic reactions not associated with anaerobes.[2] In aerobic organisms, the synthesis of monounsaturated fatty acids, tyrosine, and nicotinic acid are O_2-dependent.[3]

A general consequence of O_2-dependent biosynthesis and aerobic respiration is the production of reactive oxygenic species (ROS). When the amount of ROS in the body reaches an elevated state, significant structural modification can be observed in biological macromolecules. This state is known as "oxidative stress", and results in loss of function and degradation. Oxidative stress is a common feature in the mechanisms that cause carcinogenesis, tumor promotion, Parkinson's disease, and Alzheimer's disease, and is also implicated in the aging process.[4−9]

The superoxide radical anion ($O_2^{-\bullet}$), the perhydroxyl radical ($HO_2^{\bullet}$), and the hydroxyl radical ($HO^{\bullet}$) comprise the biologically relevant oxygen radicals.[10] Hydrogen peroxide (H_2O_2) is another biologically active oxygen species. Superoxide is formed when the ground-state O_2 molecule accepts a single electron into one of its π^* antibonding orbitals and is formed in almost all aerobic cells.[11] The addition of the subsequent electron forms the peroxide ion (O_2^{2-}), which has no unpaired electron and is not a radical and readily accepts two protons to form H_2O_2. Homolytic cleavage of the O−O bond in H_2O_2 produces two hydroxyl radicals. It has been shown that $HO^{\bullet}$ can be produced by heat, ionization radiation, or in several reactions with Fe^{2+}.[12] The hydroxyl radical reacts with an extremely high rate constant with carbohydrates, amino acids, phospholipids DNA bases, and organic acids.[12] $HO_2^{\bullet}$ is produced in reactions between $H^{\bullet}$ and O_2; however, $HO_2^{\bullet}$ has a pK_a of 4.8, therefore the biological significance of this radical may be limited.[11]

Received: March 12, 2011
Revised: May 20, 2011
Published: May 20, 2011

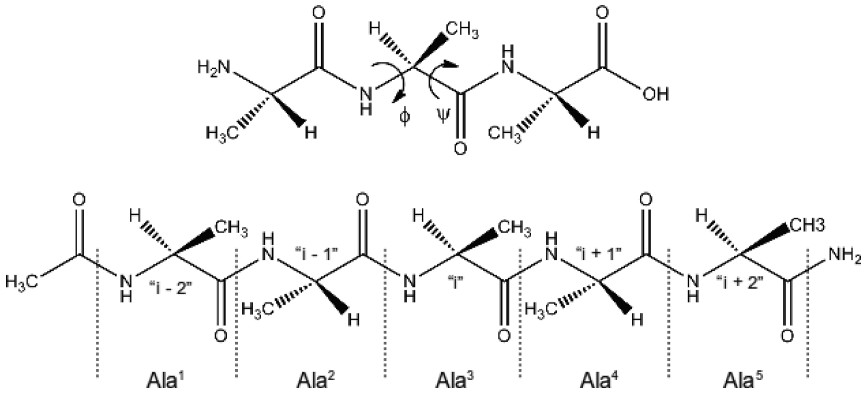

Figure 1. Representations of the ϕ and ψ nomenclature for the peptide dihedral angles (top) and the "i − 1", "i", and "i + 1" nomenclature of amino acid residues of A5 (*N*-Ac-AAAAA-NH_2).

ROS can oxidize lipids, DNA and form glycation end-products; however, proteins form by far the largest mass of oxidizable organic components of living matter.[13−16] Free radicals have been shown to induce the formation of bityrosine-induced protein aggregates, increase the rate of protein fragmentation, and increase the susceptibility of proteins to degradation.[10,17] The formation of protein carbonyls has become the marker used to identify proteins that have been damaged by oxidative stress.[18,19] All amino acids are susceptible to modification by both $HO^•$ and $HO^• + O_2^{-•}$; however, tryptophan, tyrosine, histidine, and cysteine showed greater sensitivity, and the rate of oxidation depended on the concentration of the ROS. Moreover, it was suggested that $HO^•$ is the primary radical responsible for all amino acid modifications, and that O_2^- and O_2 can further transform the products of $HO^•$ reactions.[18,20−22] A decrease in protein solubility, used as a measure of protein unfolding, was also shown in the presence of $HO^•$ in a dose-dependent manner, which was also exacerbated in the presence of O_2 and O_2^-.[23]

In the search of a subset of the Protein Data Bank, it was observed that the 3_{10}-helix occurs less frequently than the α-helix in regions that are greater than five residues, but is more prevalent in regions containing five residues or less.[24,25] Also, 3_{10}-helices are considered to be sequential type III β-turns, therefore the occurrence of these structures can be underestimated.[26,27] these short 3_{10}-helices can be crucial motifs that mediate the conformational transitions of proteins.[28−30] It has been observed that 3_{10}-helices are an intermediate structure in the conversion of α-helices to β sheets in amyloid fibrils, and this has been shown to be initiated by free radicals.[31] The aim of this study is to understand how free radicals initiate the unfolding of the 3_{10}-helix to an extended conformation.

In this study, the structural perturbations induced by hydrogen abstraction from a model pentapeptide was investigated. The B3LYP density functional was used to compare the geometries of *N*-Ac-AAAAA-NH_2 peptides with radicals centered at the C_α, C_β, and amide nitrogen atoms of Ala^3, to that of the closed-shell *N*-Ac-AAAAA-NH_2. Density functionals have been shown to lead to accurate predictions for the energetics of H-atom abstraction reactions and has also been shown to compute geometries that are in good agreement with experimentally determined values.[32,33] The penta-alanyl helix was chosen because Ala is the smallest amino acid residue that is able to stabilize the conformations preferred by L-amino acids, and its small size causes a low entropy loss, which enables helix formation.[34]

2. METHODS

The Gaussian 09 program package was used to optimize the *N*-Ac-AAAAA-NH_2 (A5) geometries. The A5 structures were optimized in the gas phase and in an implicit solvent using the unrestricted Becke three-parameter Lee−Yang−Parr (B3LYP) density functional method, with the 6-31G(d) and 6-311+G(d,p) basis sets.[35−37] The implicit solvent was represented by a conductor-like polarizable continuum model (C-PCM) for water, with a dielectric constant (ε) of 78.39.[38] The fully extended conformation ($A5_{Ext}$) was formed using initial ϕ and ψ angles of 180°, whereas the helical conformation ($A5_{Hel}$) was stabilized by hydrogen bonds between the respective amide hydrogen and carbonyl oxygen of residues "i" and "i + 2". The geometry of both structures were subsequently optimized, and their frequencies were computed to confirm that they were minima. Figure 1 illustrates the definition of the ϕ, ψ and "i" symbols used to describe peptide structure. The thermodynamic functions were calculated using the unscaled frequencies.

A hydrogen atom was removed from the C_α, CH_3 and amide nitrogen of Ala^3 in A5 to construct the $A5(C_\alpha^•)$, $A5(CH_3^•)$, and $A5(N^•)$ radicalized peptides. The geometries of $A5(C_\alpha^•)$, $A5(CH_3^•)$, and $A5(N^•)$ were subsequently optimized in the doublet electron configuration using the levels of theory, conformations, and environments used to optimize A5. The bond lengths, ϕ and ψ dihedral angles pertaining to Ala^3, hydrogen bond distances, and root-mean-squared deviations (rmsd) of peptide backbone atoms of $A5(C_\alpha^•)$, $A5(CH_3^•)$, and $A5(N^•)$ were compared to those of A5 in the case of both $A5_{EXT}$ and $A5_{HEL}$. A schematic representation of these peptide structures is shown in Figure 2.

The ΔH^o, ΔG^o, and ΔS^o for the reactions with $HO^•$, $HO_2^•$, and $O_2^{-•}$ that resulted in the formation of $A5(C_\alpha^•)$, $A5(CH_3^•)$, and $A5(N^•)$ peptide radicals were measured using the previously described gas phase and implicit solvent conditions. A diagram depicting these reactions can be found in Figure 3. The relative stability and the ΔH^o, ΔG^o, and ΔS^o of the unfolding of the peptide radicals were also computed in these conditions.

3. RESULTS

3.1. Geometric Deviations from the A5 Structure. *3.1.1. The Effect of H-Abstraction from the C_α of Ala^3.* The removal of the hydrogen atom from the C_α of $A5_{EXT}$ decreased the length of the bonds between the C_α and the amide nitrogen, methyl carbon

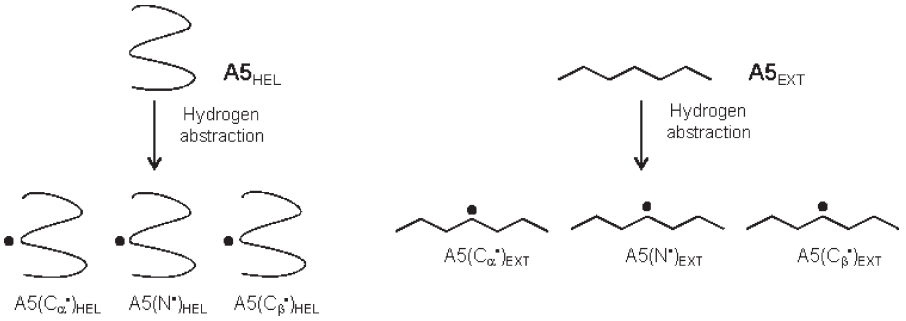

Figure 2. A schematic representation of the peptides computed in this study. The structures of the $A5_{HEL}$ and $A5_{EXT}$ peptides are to be compared to the structures of the respective peptide radicals after hydrogen abstraction.

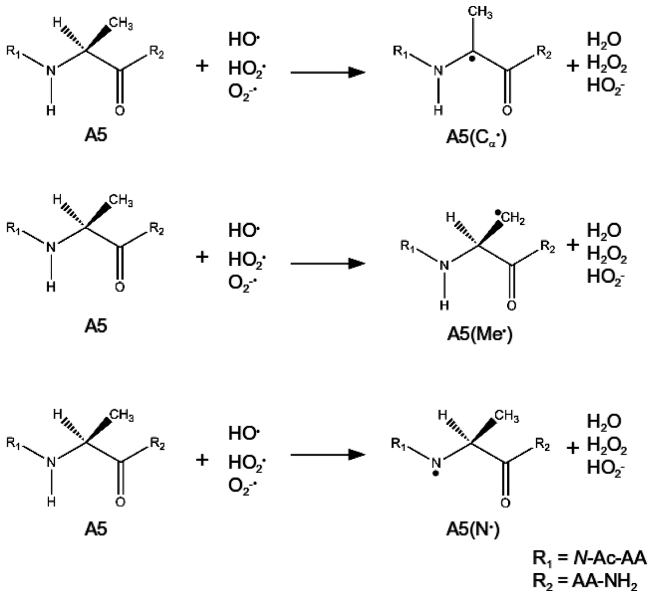

Figure 3. Schematic reaction of the A5 peptide with $HO^{\bullet}$, $HO_2^{\bullet}$, and $O_2^{-\bullet}$ yielding the A5($C_\alpha^{\bullet}$), A5($Me^{\bullet}$), or A5($N^{\bullet}$) and H_2O, H_2O_2, and HO_2^{-}.

(C_β), and carbonyl carbon atoms in the gas phase by 0.074 Å, 0.049 Å, and 0.072 Å, respectively (Table 1). The observed decrease in bond length was slightly less pronounced when the 6-31G(d) basis set was used. The length of the amide bond between Ala^3 and Ala^2 increased by 0.020 Å, whereas the length of the bond between Ala^3 and Ala^4 increased by 0.012 Å. The respective amide bonds increased by 0.024 Å and 0.013 Å when the structures were optimized in the implicit solvent.

The pleats in the $A5_{EXT}$ peptide in the extended conformation can be shown in Figure 4, and is also characterized by ϕ and ψ angles of −157.42° and 164.65°. The removal of the hydrogen atom from the C_α caused the dihedral angles to become more planar, with ϕ and ψ angles of 177.66° and −177.89°, respectively. The increased planarity was observed only at the Ala^3 of the $A5(C_\alpha^{\bullet})_{EXT}$ peptide, whereas the remaining residues retained the pleats shown in the $A5_{EXT}$ peptide. The intramolecular hydrogen bond between the amide nitrogen and the carbonyl oxygen of residue 3 decreased by 0.083 Å when the 6-311+G(d,p) basis set was used, which is 0.057 Å more than what was computed with the 6-31G(d) basis set. The rmsd of the peptide backbone containing the C_α radical from that of the $A5_{EXT}$ peptide was 0.781 Å in the gas phase, and 1.04 Å in the implicit solvent, which are shown in Table 2.

Similar to what was shown in the extended conformation, hydrogen atom abstraction from the C_α of Ala^3 increased the length of the bond between the C_α and the amide nitrogen, C_β, and carbonyl carbon atoms in the $A5_{HEL}$, as shown in Figure 5. The length of these bonds decreased by 0.062 Å, 0.042 Å, and 0.073 Å, respectively. The length of the amide bond between Ala^2 and Ala^3 increased by 0.019 Å, whereas the length of the amide bond between Ala^3 and Ala^4 increased by 0.013 Å. The respective amide bond lengths increased by 0.021 Å and 0.015 Å in the implicit solvent. Hydrogen abstraction from the C_α of residue 3 in $A5_{HEL}$ caused the ϕ dihedral angle to be more planar, as indicated by the ϕ angle changing from of −157.42° to 177.66°, however, the change in the ψ angle was negligible. This data is presented in Table 2. The hydrogen bond between the amide nitrogen of Ala^3 and carbonyl carbon of Ala^1 decreased by 0.033 Å, whereas the hydrogen bond between the carbonyl carbon of Ala^3 and the amide nitrogen of Ala^5 decreased by 0.013 Å. Changes in dihedral angles and hydrogen bond lengths suggest that there is a stronger coupling between C_α and the amide nitrogen than between the C_α and the carbonyl carbon. The rmsd of the C_α peptide radical backbone from the backbone of $A5_{HEL}$ was 0.345 Å and 0.346 Å, respectively. This data is shown in Table 2.

3.1.2. The Effect of H-Abstraction from the C_β of Ala^3. Hydrogen abstraction from the methyl group of $A5_{EXT}$ caused an increase in the length of the bond between C_β and C_α by 0.045 Å. This bond decreased by 0.042 Å in $A5_{HEL}$, as shown in Table 1. The remaining bond lengths in Ala^3 changed by less than 0.003 Å in both conformations. Moreover, the length of the amide bond between Ala^2 and Ala^3 decreased by only 0.001 Å, whereas the length of the bond between Ala^3 and Ala^4 decreased by 0.002 Å, with a negligible change shown to the respective bond lengths in optimized in the implicit solvent. The decrease in the intramolecular hydrogen bond distances in both $A5_{EXT}$ and $A5_{HEL}$ were also negligible. Also, the ϕ and ψ dihedral angles of the extended and helical A5($N^{\bullet}$) deviated from the respective $A5_{EXT}$ or $A5_{HEL}$ by less than 5° and the rmsd from the backbone of A5 was only 0.168 Å.

3.1.3. The Effect of H-Abstraction from the Amide Nitrogen of Ala^3. The removal of the hydrogen atom from the amide nitrogen caused the length of the bond between the amide N and the C_α to decrease by 0.022 Å in $A5_{EXT}$, whereas the subsequent bond between the C_α and the carbonyl carbon increased by 0.055 Å. In $A5(N^{\bullet})_{HEL}$ the decrease in the N−C_α bond length was 0.042 Å and the increase in the C_α−C═O bond length was 0.047 Å. In both conformations, the length of the amide bonds between Ala^3 and Ala^2 and those between Ala^3 and Ala^4 increased. The length of the amide

Table 1. Bond Lengths in Ala^3 of A5, A($C_\alpha^\bullet$), A($^\bullet CH_3$), and A($N^\bullet$) in the Extended and Helical Conformations[a]

		bond length (Å)						
peptide	environment	"$n-1$" amide	N−C_α	N−H	C_α−C_β	Cα−C	C═O	"$n+1$" amide
A_{Ext}	gaseous	1.350 (1.349)	1.452 (1.454)	1.015 (1.013)	1.540 (1.539)	1.539 (1.538)	1.232 (1.227)	1.350 (1.349)
	aqueous	1.345 (1.344)	1.455 (1.457)	1.015 (1.013)	1.540 (1.539)	1.538 (1.536)	1.236 (1.232)	1.345 (1.344)
$A(C_\alpha^\bullet)_{Ext}$	gaseous	1.370 (1.369)	1.379 (1.380)	1.023 (1.020)	1.494 (1.490)	1.467 (1.466)	1.247 (1.243)	1.361 (1.361)
	aqueous	1.369 (1.344)	1.379 (1.380)	1.022 (1.019)	1.494 (1.490)	1.467 (1.465)	1.251 (1.248)	1.357 (1.357)
$A(CH_2^\bullet)_{Ext}$	gaseous	1.352 (1.351)	1.459 (1.457)	1.016 (1.014)	1.459 (1.494)	1.558 (1.558)	1.231 (1.225)	1.347 (1.347)
	aqueous	1.347 (1.345)	1.456 (1.457)	1.016 (1.013)	1.496 (1.495)	1.558 (1.556)	1.234 (1.229)	1.344 (1.342)
$A(N^\bullet)_{Ext}$	gaseous	1.371 (1.371)	1.434 (1.432)		1.529 (1.529)	1.593 (1.593)	1.222 (1.216)	1.345 (1.345)
	aqueous	1.372 (1.371)	1.439 (1.440)		1.530 (1.530)	1.585 (1.581)	1.226 (1.223)	1.343 (1.342)
A_{Hel}	gaseous	1.354 (1.353)	1.460 (1.461)	1.016 (1.014)	1.531 (1.530)	1.543 (1.541)	1.232 (1.227)	1.354 (1.353)
	aqueous	1.350 (1.349)	1.458 (1.459)	1.019 (1.016)	1.533 (1.531)	1.539 (1.538)	1.239 (1.235)	1.351 (1.348)
$A(C_\alpha^\bullet)_{Hel}$	gaseous	1.373 (1.372)	1.400 (1.399)	1.020 (1.018)	1.490 (1.488)	1.470 (1.468)	1.242 (1.237)	1.367 (1.366)
	aqueous	1.371 (1.370)	1.395 (1.395)	1.022 (1.020)	1.490 (1.488)	1.465 (1.463)	1.250 (1.246)	1.364 (1.363)
$A(CH_2^\bullet)_{Hel}$	gaseous	1.353 (1.352)	1.458 (1.459)	1.015 (1.013)	1.489 (1.488)	1.562 (1.561)	1.229 (1.224)	1.353 (1.351)
	aqueous	1.350 (1.349)	1.456 (1.456)	1.018 (1.016)	1.491 (1.489)	1.557 (1.489)	1.236 (1.232)	1.350 (1.347)
$A(N^\bullet)_{Hel}$	gaseous	1.377 (1.372)	1.421 (1.419)		1.534 (1.534)	1.589 (1.588)	1.225 (1.219)	1.342 (1.342)
	aqueous	1.380 (1.374)	1.427 (1.438)		1.535 (1.538)	1.574 (1.558)	1.231 (1.226)	1.344 (1.344)

[a] The bond lengths were computed at the B3LYP/6-31G(d) and B3LYP/6-311+G(d,p) (shown in parentheses) levels of theory, both and in the gas phase and implicit solvent.

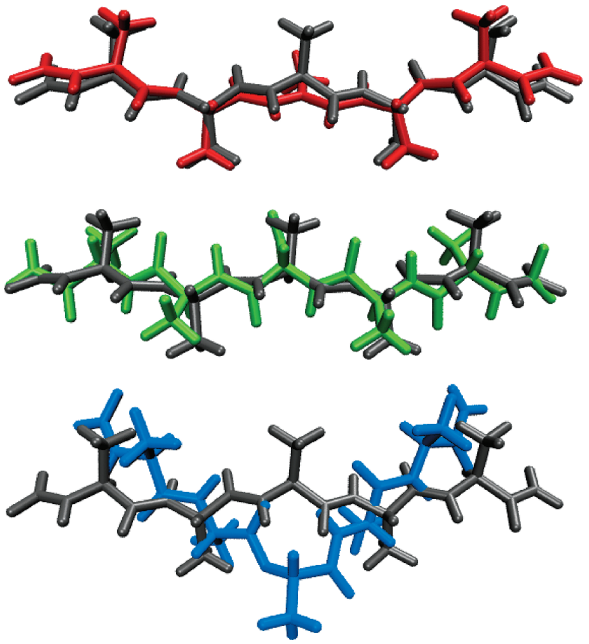

Figure 4. Structural alignment of the A5 peptide and the A5 peptide radicals in the extended conformation. The structures were obtained at the B3LYP/6-311+G(d,p) level of theory in the gas phase. The alignment of the A5($C_\alpha^\bullet$) peptide is shown in red (top), that of A5($Me^\bullet$) is shown in green (middle), and that of A5($N^\bullet$) is shown in blue (bottom), whereas the A5 peptide is shown in gray. The rmsd of the structural alignments can be found in Table 2.

bond between Ala^3 and Ala^2 increased by 0.022 Å in the extended conformation and 0.019 Å in A5($N^\bullet$)$_{HEL}$, whereas the change in the length of the amide bond between Ala^3 and Ala^4 was negligible.

In A5($N^\bullet$)$_{EXT}$, the absence of the H atom prevented the formation of the intramolecular hydrogen bond; however, a hydrogen bond was formed between the carbonyl oxygen of Ala^2 and the amide nitrogen of Ala^4. It is suspected that this contributed to the roughly 60° difference between the ϕ and ψ angles of A5$_{EXT}$ and those of A5($N^\bullet$)$_{EXT}$. In A5($N^\bullet$)$_{HEL}$, H abstraction from the amide nitrogen cleaved the hydrogen bond with the carbonyl carbon of Ala^1. The loss of the hydrogen bond resulted in a decrease in the ϕ angle by 20°. The ψ angle deviated by less than 10°. A large perturbation in structure is also shown in the rmsd value, which deviated by 2.72 Å from the backbone of A5$_{HEL}$ in the gas phase.

3.2. Thermodynamic Analysis. *3.2.1. Hydrogen Atom Abstraction Energies.* Gas phase results at the 6-311+G(d,p) basis set shows that the strength of the C_α-H bond was less than that of the C_β-H bond of the Ala side chain and that of the N−H bond of the amide group. As presented in Table 3, hydrogen abstraction from the C_α of A5$_{EXT}$ required 83.5 kJ mol^{-1} and 106.2 kJ mol^{-1} less energy than from C_β and the amide nitrogen, respectively. The difference between the bond dissociation energy (BDE) of the C_α−H bond and those of the C_β−H and N−H bonds in A5$_{HEL}$ is 58.2 kJ mol^{-1} and 92.7 kJ mol^{-1}, respectively. The BDE values of the C_α−H and N−H bonds showed a conformational dependence, as shown by the lower BDE of A5$_{HEL}$. Hydrogen abstraction from the C_α required 23.4 kJ mol^{-1} less energy in A5$_{EXT}$ than in A5$_{HEL}$, whereas hydrogen abstraction from the amide nitrogen required 9.9 kJ mol^{-1} less energy in the extended conformation.

The results obtained in the implicit solvent are within 1% of those obtained in the gas phase. The greatest deviation between the results obtained with the 6-31G(d) basis set and those obtained with the 6-311+G(d,p) basis set was shown in the A5($N^\bullet$) peptide, which had a deviation of less than 3%.

The hydrogen abstraction energy values can act as a measure of the relative peptide radical stability since each of the peptides are derived from the same reactant and have the same coproduct, an infinitely separated hydrogen atom. Therefore, the results in the gas phase with the 6-311+G(d,p) basis set indicate that

dx.doi.org/10.1021/jp202345p |J. Phys. Chem. B 2011, 115, 8014–8023

Table 2. The ϕ and ψ Dihedral Angles and H-Bond Distances of Ala^3 in A5 and the Peptide Radicals in the Extended and Helical Conformations[a]

		dihedral angle		hydrogen bond length		
peptide	environment	ϕ/degrees	ψ/degrees	amide N	carbonyl C	backbone rmsd/Å
A_{Ext}	gaseous	−160.0 (−157.4)	167.3 (164.6)	2.102 (2.114)	2.102 (2.114)	0.00 (0.00)
	aqueous	−158.5 (−152.5)	162.1 (157.4)	2.142 (2.223)	2.142 (2.223)	0.00 (0.00)
$A(C_\alpha^\bullet)_{Ext}$	gaseous	−178.7 (177.6)	−179.5 (−177.8)	2.022 (2.031)	2.022 (2.031)	0.673 (0.781)
	aqueous	178.1 (172.9)	178.9 (−177.2)	2.04 (2.068)	2.04 (2.068)	0.854 (1.04)
$A(^\bullet CH_3)_{Ext}$	gaseous	−164.4 (−160.6)	−163.1 (171.5)	2.064 (2.108)	2.064 (2.108)	0.0623 (0.168)
	aqueous	−163.1 (−159.0)	169.2 (161.0)	2.102 (2.171)	2.102 (2.171)	0.192 (0.143)
$A(N^\bullet)_{Ext}$	gaseous	−98.2 (−98.6)	66.0 (72.6)			2.72 (2.53)
	aqueous	−100.7 (−102.5)	67.0 (69.1)			2.59 (2.43)
A_{Hel}	gaseous	−63.2 (−64.6)	−19.9 (−18.4)	2.107 (2.183)	2.15 (2.176)	0.00 (0.00)
	aqueous	−61.1 (−63.2)	−24.3 (−20.9)	2.068 (2.171)	2.082 (2.115)	0.00 (0.00)
$A(C_\alpha^\bullet)_{Hel}$	gaseous	−45.5 (−45.9)	−21.6 (−22.4)	2.074 (2.127)	2.137 (2.176)	0.352 (0.345)
	aqueous	−45.0 (−45.6)	−22.0 (−22.7)	2.039 (2.129)	2.04 (2.083)	0.421 (0.346)
$A(^\bullet CH_2)_{Hel}$	gaseous	−61.3 (−62.2)	−24.4 (−22.5)	2.112 (2.173)	2.193 (2.213)	0.0973 (0.0667)
	aqueous	−59.7 (−60.8)	−26.8 (−24.3)	2.065 (2.151)	2.083 (2.123)	0.0547 (0.0324)
$A(N^\bullet)_{Hel}$	gaseous	−80.1 (−81.4)	−11.3 (−12.5)		2.264 (2.302)	0.645 (0.524)
	aqueous	−81.5 (−86.0)	−13.6 (−22.9)		2.176 (2.153)	0.654 (1.25)

[a] The geometric parameters were computed at the B3LYP/6-31G(d) and B3LYP/6-311+G(d,p) (shown in parentheses) levels of theory, both in the gas phase and implicit solvent. The rmsd of the backbone atoms for the peptide radicals compared to those of A5 is also shown.

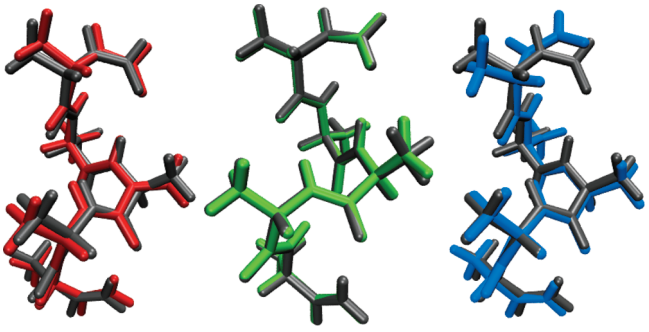

Figure 5. Structural alignment of the A5 peptide and the A5 peptide radicals in the helical conformation. The structures were obtained at the B3LYP/6-311+G(d,p) level of theory in the gas phase. The alignment of the $A5(C_\alpha^\bullet)$ peptide is shown in red (left), that of $A5(Me^\bullet)$ is shown in green (middle) and that of $A5(N^\bullet)$ is shown in blue (right), whereas the A5 peptide is shown in gray. The rmsd of the structural alignments can be found in Table 2.

$A5(C_\alpha^\bullet)_{EXT}$ is 83.5 kJ mol^{-1} more stable than $A5(CH_2^\bullet)_{EXT}$ and 106.2 kJ mol^{-1} more stable than $A5(N^\bullet)_{EXT}$. The relative stabilities computed in the implicit solvent model are within 1% of the gas phase values, and a similar deviation was observed between the two basis sets. $A5(C_\alpha^\bullet)_{EXT}$ is 58.2 kJ mol^{-1} more stable than $A5(^\bullet CH_3)_{EXT}$ and 92.7 kJ mol^{-1} more stable than $A5(N^\bullet)_{EXT}$. As shown in the extended conformation, the deviations from the relative stability values were negligible when the implicit solvent and the smaller basis set were used.

3.2.2. Helical Unfolding. The change in standard free energy (ΔG^o) for the unfolding of $A5_{HEL}$, $A5(C_\alpha^\bullet)_{HEL}$, $A5_{HEL}(CH_2^\bullet)$, $A5(N^\bullet)_{HEL}$, calculated with the 6-311+G(d,p) basis set, are all negative when computed in the gas phase. Moreover, the changes in the standard entropy (ΔS^o) for the unfolding of these peptides were all positive, which indicates that the unfolding is entropy-driven. These results can be found in Table 3. The ΔG^o for the unfolding of $A5(CH_2^\bullet)_{HEL}$ and $A5(N^\bullet)_{HEL}$ are similar to that of $A5_{HEL}$; however, the unfolding of $A5(C_\alpha^\bullet)_{HEL}$ is more favorable than the unfolding of $A5_{HEL}$, showing a difference in ΔG^o of −18.6 kJ mol^{-1}.

Changes in the standard enthalpy (ΔH^o) of unfolding shows that the unfolding of $A5(C_\alpha^\bullet)_{HEL}$ is 16.7 kJ mol^{-1} more exothermic than the unfolding of $A5_{HEL}$, which suggests that increased tendency of $A5(C_\alpha^\bullet)_{HEL}$ to unfold is also enthalpy-driven. The unfolding of $A5(N^\bullet)_{HEL}$ is 8.7 kJ mol^{-1} more exothermic than the unfolding of the $A5_{HEL}$ peptide. Moreover, the unfolding of $A5(C_\alpha^\bullet)_{HEL}$ and $A5(N^\bullet)_{HEL}$ is associated with a smaller increases in entropy than the unfolding of $A5_{HEL}$, by 9.4 J mol^{-1}K^{-1} and 23.2 J mol^{-1}K^{-1}, respectively. As shown by the ΔG^o values, the unfolding of each peptide was less favorable in the implicit solvent than in the gas phase.

3.2.3. Reactions of $A5_{Ext}$ and $A5_{Hel}$ with ROS. The change in free energy computed in the gas phase with the 6-311+G(d,p) basis set showed that only the reactions involving the $HO^\bullet$ radical and $A5_{EXT}$ were exergonic. These results can be found in Table 4. For reactions at the C_α of $A5_{EXT}$ in the gas phase, the reactions involving the $HO^\bullet$ radical required 167.2 kJ mol^{-1} more free energy than those with the $HO_2^\bullet$ radical and 226.3 kJ mol^{-1} more free energy than with the $O_2^{-\bullet}$ radical. The reaction Gibbs free energy values indicate that the C_α is more susceptible than the C_β and amide nitrogen to H-abstraction by the ROS. The reaction of $HO^\bullet$ with $A5_{EXT}$ at the C_α required 79.3 kJ mol^{-1} more free energy than the abstraction from the CH_3 and 102.4 kJ mol^{-1} more energy than the abstraction from the amide nitrogen. The ΔH^o values of the reactions with each of the ROS were similar to those of the ΔG^o values. The H abstraction reactions of each ROS in the gas phase gained entropy, irrespective of the location. Hydrogen abstraction from C_α and the amide nitrogen showed a decrease of enthalpy in the implicit solvent, whereas the reactions with $O_2^{-\bullet}$ radical showed the largest gain in entropy. Results in the gas phase with the 6-311+G(d,p) basis set showed that the reaction of the

Table 3. Reactions of $^{\bullet}OH$, $HO_2^{\bullet}$, and $O_2^{-\bullet}$ with A5 in the Helical and Extended Conformations[a]

		H abstraction energy (kJ mol^{-1})		transition from helical to extended		
peptide	environment	extended	helix	ΔH^o (kJ mol^{-1})	ΔG^o (kJ mol^{-1})	ΔS^o (J mol^{-1} K^{-1})
A5	gaseous			10.8 (2.3)	−7.8 (−17.8)	62.8 (67.9)
	aqueous			29.5 (15.2)	9.0 (−7.3)	68.6 (75.5)
A5($C_\alpha^{\bullet}$)	gaseous	366.4 (367.5)	393.0 (390.9)	−13.4 (−19.0)	−27.7 (−36.4)	48.1 (58.5)
	aqueous	369.2 (370.4)	390.0 (387.6)	9.2 (0.0)	−14.2 (−18.4)	78.8 (61.6)
A5($^{\bullet}CH_2$)	gaseous	456.9 (451.0)	455.2 (449.1)	12.7 (4.5)	−6.6 (−16.6)	65.0 (70.8)
	aqueous	455.6 (449.3)	455.6 (450.1)	29.1 (14.4)	8.5 (−9.1)	68.9 (79.1)
A5($N^{\bullet}$)	gaseous	461.4 (473.7)	475.9 (483.6)	−2.5 (−6.4)	−13.1 (−19.7)	35.6 (44.7)
	aqueous	463.8 (476.6)	489.1 (486.6)	4.1 (5.2)	−8.9 (−3.2)	43.7 (28.6)

[a] The free energy of H abstraction and helical to extended unfolding are computed at the B3LYP/6-31G(d) and B3LYP/6-311+G(d,p) levels (in parentheses).

$O_2^{-\bullet}$ radical at the C_α of the $A5_{EXT}$ yielded 10.7 J·mol^{-1}K^{-1} and 21.1 J·mol^{-1}K^{-1} more entropy than the analogous reaction with $HO^{\bullet}$ and $O_2^{-\bullet}$.

The order of the reactivity of the ROS with $A5_{HEL}$ was qualitatively similar to those with $A5_{EXT}$; however, the ΔG^o of each reaction was slightly less favorable. Moreover, the relative ease at which a hydrogen atom can be abstracted from the C_α, C_β, and the amide nitrogen of $A5_{HEL}$ was also similar to what was found in $A5_{EXT}$.

4. DISCUSSION

4.1. Geometric Deviations from the A5 Structure. *4.1.1. Structural Perturbations due to C_α-Hydrogen Atom Abstraction.* The stability of planar conformations in C_α radicals has been shown previously by Himo and co-workers; however, the effect of this phenomenon on the structure of the 3_{10} helix and the fully extended conformation of a pentapeptide has not been shown.[39,40] The density functional methods used herein enable the effects of long-range interactions of helices, such as "i, i − 2" hydrogen bonds, on the geometry of the different radical structures to be determined accurately, and compared to the that of the closed shell analogue. The shift toward the β conformation (ϕ, ψ = 180°) is in agreement with that shown in a glycyl diamide model, in which the β conformation was shown to be the most stable.[41] Allyl-type radicals have a higher stability compared to nondelocalized radicals and favor the planar conformation. This structure has been shown to have a rotational energy barrier of approximately 15 kcal/mol.[42−44] The stability of this conformation can be attributed to the overlap of the semioccupied π-orbital of the radical with the p-orbitals of the amide nitrogen and carbonyl carbon. This structure can stabilize the C_α radical due to the conjugation between the nitrogen atom of the amide and carbon atom of the carbonyl group, which has also been shown previously in cyclic and amino alkyl compounds.[45,46] Further evidence of the delocalization is the decreased length of the N−C_α and C_α−C bonds, which indicates an increase in double-bond character. The increase in the C_α−C bond length was observed in the extended structure, but not in the helix, indicative of the tendency of the helix to inhibit the delocalization of the unpaired electron. The increased length of the amide bonds between Ala^2 and Ala^3 and the amide bond between Ala^3 and Ala^4 indicates that these bonds become more like single bonds, which are weaker and are more susceptible to enzymatic degradation and peptide fragmentation.

The stabilization of the radical by the amide nitrogen is 2-fold, due to the electron-donating properties of the amide nitrogen, and the ability of the amide bond to delocalize the unpaired electron.[47] The stronger $C_\alpha^{\bullet}$ coupling to the amide nitrogen than to the carbonyl carbon is shown in the larger change in bond length in A5($C_\alpha^{\bullet}$). The increased planarity is shown by the lack of pleats in the extended conformation (Figure 4) at the Ala^3 position, and ϕ and ψ angles of nearly 180°. Planarity of the atoms in Ala^3 was also shown in $A5_{HEL}$ (Figure 5), with both the ϕ and ψ angles approaching 0° (Table 2). It can be observed that this effect does not carry over to Ala^2 or Ala^4 in either $A5_{EXT}$ or $A5_{HEL}$.

4.1.2. Structural Perturbations due to C_β-Hydrogen Atom Abstraction. The change in length of the amide bond between adjacent residues is indicative of the coupling between the methyl group and the resonance structures of the amide bond.[48] However, compared to the effect of radical formation on the C_α and amide nitrogen on the peptide structures, this coupling is relatively weak. Apart from the length of the C_α−C_β bond, C_β-radical formation had a negligible effect on the bond lengths, dihedral angles, or hydrogen bonds of either $A5_{EXT}$ or $A5_{HEL}$. The methyl group of Ala is the β-CH_2 of the other amino acids apart from glycine, and it is expected that radical formation at this or any other position of the side chain would have negligible inductive effects on the conformation of the peptide backbone. Moreover, the effect on the length of the amide bond is negligible, suggesting that side chain oxidation does not cause the peptide bond to weaken.

4.1.3. Structural Perturbations due to Amide Nitrogen−Hydrogen Atom Abstraction. Numerous theoretical studies have been done on hydrogen atom abstraction from the free amino group, with some suggesting the that the amino hydrogen is the preferred target by $HO^{\bullet}$.[49−51] However, when the amide nitrogen is derivatized, it was shown that reactions at the side chain are always preferred.[52] Although free amino acids and their derivatives can provide a good description of local electronic effects, hydrogen abstraction from the amide bond of model peptides help determine the effect of long-range interactions and hydrogen bonding. The removal of a hydrogen atom showed an increase of the amide bond length with the adjacent carbonyl carbon, along with the an increase in the length of the C_α−C bond. The N−C_α bond length decreased, which is consistent with the formation of an imine.[53]

The most significant effect of the H-atom abstraction from the amide nitrogen is due to the rearrangement of the hydrogen

dx.doi.org/10.1021/jp202345p |J. Phys. Chem. B 2011, 115, 8014–8023

bonds. Instead of the hydrogen bond between the amide nitrogen and carbonyl oxygen of residue 3 in the extended conformation, a hydrogen bond formed between the carbonyl oxygen of the Ala^2 and the amide hydrogen of Ala^4. It is presumed that this caused the observed deviation in the ϕ and ψ dihedral angles in this structure compared to that of the A5 extended ϕ and ψ angles. In the helical conformation, the removal of the Ala^3 amide hydrogen eliminated the hydrogen bond that was formed with this residue and the Ala^1 carbonyl carbon. The observed increase in the amide bond length suggests that $N^{\bullet}$-containing peptides can be more labile than in a peptide without a radical.

The rmsd values indicate that the H abstraction from the C_β did not significantly change the structure of A5. H abstraction from the C_α increased the planarity of the peptide, but the secondary structure of the peptide remained intact, whereas H abstraction from the amide nitrogen altered the secondary structure of the peptide.

4.2. Thermodynamic Analysis. *4.2.1. BDE and Peptide Radical Stability.* It is expected that with the increase in the number of delocalized electrons in the conjugated system, the stability of the radical will increase.[54] It is likely that this phenomenon contributes to the lower dissociation energy of the C_α−H bond compared to that of the C_β−H and N−H bonds. The lower relative BDE of $A5_{EXT}$ compared to that of $A5_{HEL}$ is similar to results shown by others; however, the secondary structures were mimicked with the use of smaller peptide fragments.[55−57] The use of a pentapeptide enables the inclusion intramolecular hydrogen effects of the secondary structural elements. The conformational dependence shown in the smaller fragments was shown to be less in the pentapeptide computed herein, suggesting that the diamide models may exclude the stabilization effect of intramolecular hydrogen bonding. The similarity of the BDE results computed at the 6-31G(d) and 6-311+G(d,p) basis sets indicate that the inclusion of diffuse functions and polarizable functions on hydrogen did not significantly improve the BDE values. It is possible that captodative stabilization and the larger number of delocalized electrons of the $A5(C_\alpha)$ are reasons for the relative stability. These results also agree with experimental results that state that $HO^{\bullet}$ attack at the C_α position of Ala peptides is favored over C_β.[50,52]

4.2.2. Helical Unfolding. The use of computational chemistry enables the stability of radicals at different sites of the same compound to be measured, which enables the relative stability of otherwise transient structures to be evaluated. This information can help measure the thermodynamic functions and determine the stability of folding intermediates, which can provide insight into unfolding mechanisms. Here, the ΔG° values indicate that the unfolding of the A5 peptide from a 3_{10}-helix to the $A5_{EXT}$ radical is favorable, but much more so when there is a C_α present on Ala^3. The ΔG° for the unfolding of $A5(C_\beta^{\bullet})_{HEL}$ and $A5(N^{\bullet})_{HEL}$ suggests that the propensity of these structures to unfold is not significantly greater than the propensity of $A5_{HEL}$. It has been shown that radical formation on peptides causes peptides and proteins to unfold, and it has been hypothesized as a possible mechanism for the aggregation of amyloid peptides.[58,59] These results indicate that the unfolding of $A5_{HEL}$ is more favorable when a C_α radical is present. If a radical was to form at the C_β or amide nitrogen, then a hydrogen transfer reaction is likely to preclude unfolding. According to several experimental studies, intermolecular hydrogen transfer reactions almost exclusively result in the formation of C_α radicals.[60−62] The unfolding of all the peptides result in an increase in entropy, which can also cause peptides and proteins to unfold.

Table 4. The Enthalpy, Free Energy and Entropy of the Reactions of $^{\bullet}OH$, $HO_2^{\bullet}$, and $O_2^{-\bullet}$ with A5, Producing the $A(C_\alpha^{\bullet})$, $A(^{\bullet}CH_3)$, and $A(N^{\bullet})$ Radicals in the Helical and Extended Conformations[a]

		ΔH° (kJ mol^{-1})			ΔG° (kJ mol^{-1})			ΔS° (J mol^{-1} K^{-1})		
reactants	environment	C_α	CH_3	N	C_α	CH_3	N	C_α	CH_3	N
$OH^{\bullet} + A5_{Ext}$	gaseous	−138.4 (−140.9)	−52.7 (−61.6)	−47.4 (−38.5)	−123.4 (−145.8)	−40.3 (−69.1)	−32.9 (−44.2)	14.9 (16.6)	23.6 (25.1)	16.8 (19.2)
	aqueous	−124.0 (−145.0)	−41.7 (−70.7)	−32.4 (−42.4)	−131.6 (−145.3)	−46.8 (−76.4)	−36.6 (−42.4)	25.6 (0.9)	17.2 (19.3)	14.0 (0.1)
$HO_2^{\bullet} + A5_{Ext}$	gaseous	16.0 (26.3)	101.7 (105.6)	107.0 (128.7)	46.9 (24.4)	130.0 (101.2)	137.4 (126.0)	4.4 (6.2)	13.1 (14.8)	6.3 (8.9)
	aqueous	33.7 (12.6)	116.0 (87.0)	125.2 (115.2)	29.2 (15.4)	114.0 (84.3)	124.2 (118.3)	15.1 (−9.4)	6.7 (9.0)	3.5 (−10.2)
$O_2^{-\bullet} + A5_{Ext}$	gaseous	83.5 (85.4)	169.3 (164.7)	174.6 (187.8)	75.9 (77.2)	159.0 (154.0)	166.4 (178.8)	25.6 (27.3)	34.2 (35.9)	27.4 (30.0)
	aqueous	86.5 (89.6)	168.8 (164.0)	178.1 (192.3)	75.7 (86.2)	160.5 (155.0)	170.7 (189.0)	36.2 (11.5)	27.8 (30.0)	24.5 (10.7)
$OH^{\bullet} + A5_{Hel}$	gaseous	−114.2 (−119.5)	−54.6 (−63.7)	−34.0 (−29.7)	−103.5 (−127.2)	−41.5 (−70.3)	−27.6 (−42.3)	29.6 (26.0)	21.3 (22.3)	43.9 (42.5)
	aqueous	−103.7 (−129.7)	−41.3 (−69.9)	−7.0 (−32.4)	−108.3 (−134.1)	−46.3 (−74.6)	−18.6 (−46.4)	15.5 (14.8)	17.0 (15.8)	38.9 (47.0)
$HO_2^{\bullet} + A5_{Hel}$	gaseous	40.3 (47.7)	99.8 (103.5)	120.5 (137.5)	66.8 (43.0)	128.8 (99.9)	142.7 (127.9)	19.1 (15.7)	10.8 (11.9)	33.5 (32.2)
	aqueous	54.0 (27.9)	116.4 (87.7)	150.6 (125.2)	52.5 (26.5)	114.5 (86.1)	142.1 (114.3)	5.0 (4.4)	6.5 (5.4)	28.4 (36.6)
$O_2^{-\bullet} + A5_{Hel}$	gaseous	107.8 (106.8)	167.3 (162.6)	188.0 (196.6)	95.8 (95.8)	157.8 (152.7)	171.7 (180.7)	40.2 (36.8)	32.0 (33.0)	54.6 (53.2)
	aqueous	106.8 (104.9)	169.3 (164.7)	203.5 (202.2)	99.1 (97.3)	161.0 (156.8)	188.7 (185.0)	26.1 (25.4)	27.6 (26.4)	49.5 (57.6)

[a] The values were computed in the gas phase and implicit solvent, at the B3LYP/6-31G(d) and B3LYP/6-311+G(d,p) (in parentheses) levels of theory.

dx.doi.org/10.1021/jp202345p | J. Phys. Chem. B 2011, 115, 8014–8023

Therefore, radical-initiated unfolding is likely to be a result of the formation of the C_α radical.

4.2.3. Reactions of A5 with ROS. The results in a model peptide indicate that hydrogen abstraction by the $HO^\bullet$ radical is favorable from each of the three positions, which is consistent with what was shown in model amides.[63] This study also showed that abstraction from the amide nitrogen was the least favored, which can be attributed to the relative stability of the amide bond. Hydrogen abstraction from the amide nitrogen of $A5_{HEL}$ also had the largest change in entropy. The smaller gain in entropy can be observed in $A5_{EXT}$ because the hydrogen bond in Ala^3 is replaced with a hydrogen bond between the carbonyl oxygen of Ala^3 and the amide nitrogen of Ala^2. The reaction at the C_α was the most endergonic and is enthalpy driven, due to the stabilization discussed previously. In spite of the large endergonicity, the associated gain in entropy of reactions at the C_α is less than what is calculated in the reactions at the other sites, although the differences are not significantly different from that measured at the C_β.

The reactivity of $HO^\bullet$ can be attributed to the high dissociation energy of the O−H bond in H_2O, which is 499.2 kJ mol^{-1}.[64] Accordingly, reactions with the $HO^\bullet$ radical are exergonic at the C_α, C_β and amide nitrogen sites in all conditions calculated herein. Despite being the most endergonic, the largest gain in entropy was measured in the reactions with the $O_2^{-\bullet}$ radical, which, in addition to the ΔH measured directly, indicates that the change in enthalpy was the least favorable in this ROS.

These results indicate that a hydrogen atom from the C_α, C_β, and amide nitrogen by $HO^\bullet$ but not for $HO_2^\bullet$ or $O_2^{-\bullet}$. It is well-known that the $OH^\bullet$ is the most reactive, but is has also been shown that $HO^\bullet$ is more destructive when $HO_2^\bullet$ or $O_2^{-\bullet}$ are present. A hypothesis for this phenomenon is discussed in the next section.

4.2.4. Thermodynamic Cycles of Reactions Involving the C_α of A5 and the ROS. As discussed previously, the oxidation of proteins has been shown to cause proteins to unfold. Moreover, it has been hypothesized that radical-initiated protein unfolding is the first step in the mechanism that causes the formation of the amyloid plaques, which are hallmarks of Alzheimer's, Creutzfeld-Jakob, and Parkinson's diseases. The results obtained herein allow the thermodynamic parameters of this process to be quantified and enable the propensity of the $HO^\bullet$, $HO_2^\bullet$ and $O_2^{-\bullet}$ radicals to initiate this process to be compared. The ΔH°, ΔG°, and ΔS° for the oxidation of $A5_{HEL}$ by $HO^\bullet$ are all favorable, whereas oxidation by $HO_2^\bullet$ and $O_2^{-\bullet}$ are not favorable. After the endothermic, exergonic, and entropically favorable unfolding of $A5_{Hel}^\bullet$, the ΔH° and ΔG° for the formation of the reduction of $A5_{EXT}$ by H_2O_2 and HO_2^- are all negative. Amyloid plaques are not radicals, so in this scheme, $A5_{EXT}$ is the structure that best represents the amyloid plaques that have been associated with Alzheimer's disease, and can therefore suggest a role for the H_2O_2 and HO_2^- in the formation of amyloid plaques. This scheme illustrates how each step in the unfolding of $A5_{HEL}$ is favorable when $HO^\bullet$, H_2O_2, and HO_2^- are present, as shown by Davies, et al., in which backbone cleavage and degradation by $HO^\bullet$ is exacerbated when H_2O_2 and HO_2^- are also present.[10,20,65] A schematic comparison between the radical-initiated unfolding of $A5_{HEL}$ is shown in Figure 6. The radical-initiated unfolding of a helix is more favorable than a mechanism without radical, which would likely involve less stable intermediates.

In Figure 7, competing mechanisms for the conversion of $A5_{HEL}$ to $A5_{EXT}^\bullet$ is shown. The $A5_{EXT}^\bullet$ is the form in which the oxidized peptide can propagate, causing new C_α radicalized

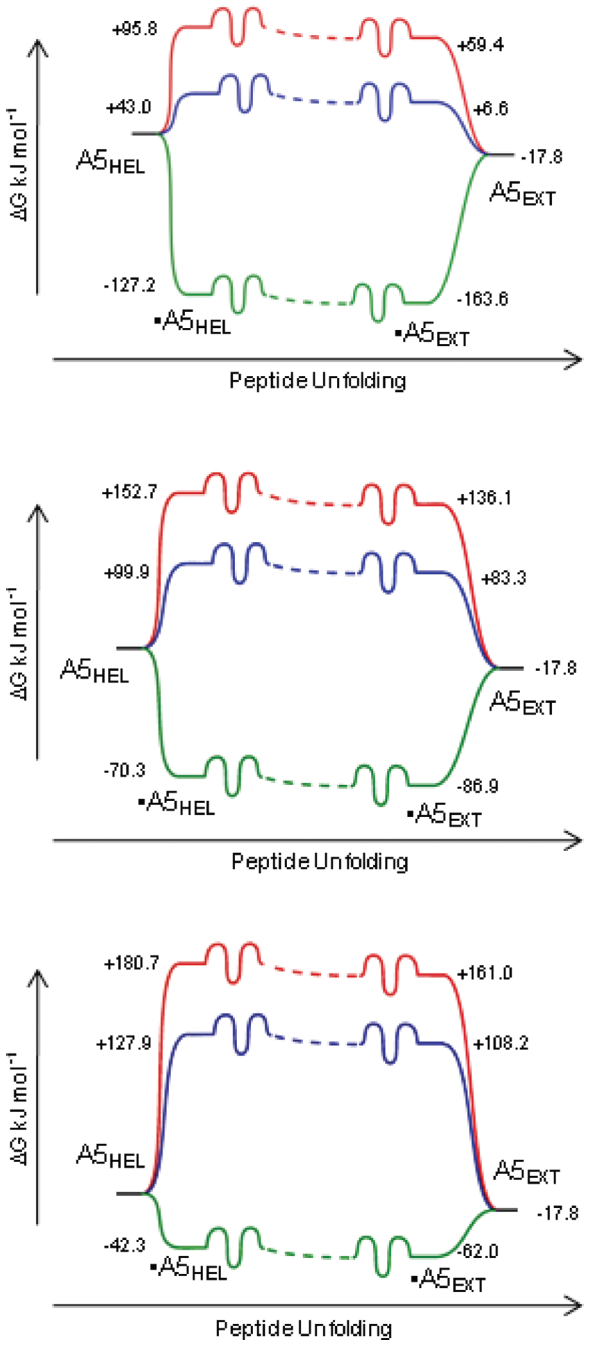

Figure 6. Schematic representations of the ΔG associated with the radical-initiated conversion of $A5_{Hel}$ to $A5_{Ext}$ by $HO^\bullet$,(green), $HO_2^\bullet$ (blue), and $O_2^{-\bullet}$ (red). In each panel the top curve is for $O_2^{-\bullet}$, the middle curve is for $HO_2^\bullet$ and the bottom curve is for $HO^\bullet$. The top panel shows the ΔG° for the reaction at the C_α, whereas the middle and bottom panels show ΔG° for H abstraction from C_β and the amide N, respectively.

peptides to form. The ΔG° of $A5_{HEL}^\bullet$ unfolding shows that $A5_{EXT}^\bullet$ is more stable, therefore, with its longer half-life, $A5_{EXT}^\bullet$ is likely to be more toxic. Amyloidogenic peptides are generally helix forming. In order to form $A5_{EXT}^\bullet$, $A5_{HEL}$ can either unfold prior to oxidation or unfold after oxidation. As shown in Figure 7, the conversion from $A5_{HEL}$ to $A5_{EXT}^\bullet$ is exergonic for both pathways when oxidized by $HO^\bullet$; however, unfolding prior to oxidation is entropy-driven, whereas oxidation prior to unfolding

dx.doi.org/10.1021/jp202345p |J. Phys. Chem. B 2011, 115, 8014–8023

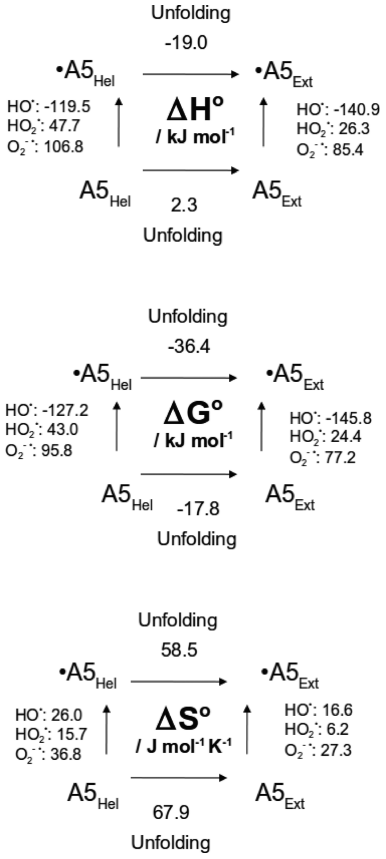

Figure 7. ΔH°, ΔG°, and ΔS° for the competing mechanisms of $A5_{Hel}$ to $^{\bullet}A5_{Ext}$ conversion initiated by H abstraction from the C_{α} of Ala^3 by $HO^{\bullet}$, $HO_2^{\bullet}$ or $O_2^{-\bullet}$. In mechanism 1 (upward from $A5_{Hel}$) the H abstraction precedes the unfolding. In mechanism 2 (to the right from $A5_{Hel}$) the unfolding precedes the H-abstraction.

is enthalpy-driven. A previous study in which the entropy per residue of homo-oligomeric peptides was measured, it was shown that there is a greater entropy per each residue added in the extended conformation than in the helical conformation.[66] The entropy contribution to the helical to extended equilibrium would favor the extended conformation in native peptides; however, it remains to be seen how peptide length will affect this equilibrium when a C_{α} radical is present.

It would be interesting to see the extent to which the unfolding shown in this study compares to what would be observed in peptide fragments in an experiment. The unfolding of the peptide could be monitored using nuclear magnetic resonance or circular dichroism spectroscopy. One of the limitations of quantum chemical calculations is the size of the system that could be studied. This could be overcome in an experiment, which could be used to observe the unfolding of larger peptides. This could be a useful area for further study.

5.0. CONCLUSIONS

In this study we have shown how a free radical can initiate the unfolding of a helical peptide. Hydrogen atom abstraction from the C_{α} of Ala^3 of *N*-Ac-AAAAA-NH_2 produces a radical that is stabilized by capto-dative and inductive effects, with no effects shown on the structure neighboring residues. The conformation of Ala^3 becomes more planar; however, the secondary structural elements are conserved. Hydrogen atom abstraction from the amide nitrogen eliminates the hydrogen bond with Ala^1 in the helix and the hydrogen bond within residue 3 in $A5_{EXT}$. The structural perturbations of the peptide containing the C_{β} radical are negligible. An increase in the length of the amide bond is shown when the C_{α} and amide nitrogen radicals are formed, suggestive of an decrease in bond stability, which is not observed when a radical forms at C_{β}.

The hydrogen abstraction reaction energies indicate that the C_{α} radical is the most stable, whereas the radical at the amide nitrogen is the least. The ΔG values for the transition from the 3_{10}-helix to the extended conformation indicated that the unfolding of $A5(C_{\alpha}^{\bullet})_{HEL}$ is the most favorable, followed by the $A5(N^{\bullet})_{HEL}$, whereas the propensity of $A5(N^{\bullet})_{HEL}$ and $A5(C_{\beta})_{HEL}$ to unfold is similar to that of $A5_{HEL}$. The secondary structure of a peptide has a strong influence on the H$-C_{\alpha}$ bond, but not the H$-C_{\beta}$, nor the N$-$H, which can protect the protein from radical-initiated hydrogen abstraction. Hydrogen abstraction by $HO^{\bullet}$ radical is the most favorable of the ROS studied, followed by $HO_2^{\bullet}$ and $O_2^{-\bullet}$.

Thermodynamic cycles of the A5 reactants and products of hydrogen abstraction indicate that the conversion of $A5_{Hel}$ to $A5_{Ext}^{\bullet}$ is exergonic, exothermic, and entropically favorable. Therefore, the radical-initiated unfolding of $A5_{HEL}$ is endothermic when initiated by $OH^{\bullet}$ and terminated by a reducing agent. This work provides new insight into the unfolding mechanism of peptides in the cellular condition known as oxidative stress.

■ ASSOCIATED CONTENT

Supporting Information. The potential energy, thermal energy, enthalpy, free energy and entropy of all the compounds computed in this study. This material is available free of charge via the Internet at http://pubs.acs.org.

■ AUTHOR INFORMATION

Corresponding Author

*E-mail: viskolcz@jgypk.u-szeged.hu. Phone: (36-62) 544720. Fax: (36-62) 420953.

■ ACKNOWLEDGMENT

We thank László Müller and Máté Labádi for the administration of the computing systems used for this work. We also thank Milán Szőri for his helpful discussion. This work was supported by TAMOP4.2.1/B-09-1/KNOV-210-0005.

■ ABBREVIATIONS

ROS, reactive oxygen species; DFT, density functional theory; C-PCM, B3LYP, conductor-like polarizable continuum model; rmsd, root mean squared deviation

■ REFERENCES

(1) Falkowski, P. G. *Science* **2006**, *311*, 1724–1725.
(2) Raymond, J; Segré, D. *Science* **2006**, *311*, 1764–1767.
(3) Goldfine, H. *J. Gen. Physiol.* **1965**, *49*, 253–274.
(4) Cohen, S. M. *Environ. Health Perspect.* **1983**, *50*, 51–59.
(5) Kobliashev, V. A. *Biochemistry (Moscow)* **2010**, *75*, 675–685.
(6) Fatehi-Hassanabad, Z.; Chan, C. B.; Furman, B. L. *Eur. J. Pharmacol.* **2010**, *636*, 8–17.
(7) Jenner, P. *Ann. Neurol.* **2003**, *53* (Suppl 3), S26–S36.

(8) Barnham, K. J.; Masters, C. L.; Bush, A. I. *Nat. Rev. Drug Discovery* **2004**, *3*, 205–214.
(9) Stadtman, E. R. *Free Radical Res.* **2006**, *40*, 1250–1258.
(10) Davies, K. J. A. *J. Biol. Chem.* **1987**, *262*, 9895–9901.
(11) Fridovich, I. *Annu. Rev. Biochem.* **1975**, *44*, 147–159.
(12) Halliwell, B.; Gutteridge, M. C. *Biochem. J.* **1984**, *219*, 1–14.
(13) Spiteller, G. *Free Radical Biol. Med.* **2006**, *41*, 362–387.
(14) Dizdaroglu, M. *Mutat. Res.* **1992**, *275*, 331–342.
(15) Fu, M. X.; Wells-Knecht, K. J.; Blackedge, J. A.; Lyons, T. J.; Thorpe, S. R.; Baynes, J. W. *Diabetes* **1994**, *43*, 676–683.
(16) Gebicki, J. M.; Nauser, T.; Domazou, A.; Steinmann, D.; Bounds, P. L.; Koppenol, W. H. *Amino Acids* **2010**, *39*, 1131–1137.
(17) Willix, R. L.; Garrison, W. M. *Radiat. Res.* **1967**, *32*, 452–462.
(18) Garrison, W. M.; Jayco, M. E.; Bennett, W. *Radiat. Res.* **1962**, *17*, 341–352.
(19) Levine, R. L. *J. Biol. Chem.* **1983**, *258*, 11823–11827.
(20) Davies, K. J. A.; Delsignore, M. E.; Lin, S. W. *J. Biol. Chem.* **1987**, *262*, 9902–9907.
(21) Prütz, W. A.; Butler, J.; Land, E. J. *Int. J. Radiat. Biol.* **1983**, *44*, 183–196.
(22) Schuessler, H.; Schilling, K. *Int. J. Radiat. Biol.* **1983**, *45*, 267–281.
(23) Davies, K. J. A.; Delsignore, M. E. *J. Biol. Chem.* **1987**, *262*, 9908–9913.
(24) Barlow, D. J.; Thornton, J. M. *J. Mol. Biol.* **1988**, *201*, 601–619.
(25) Biron, Z.; Khare, S.; Samson, A. O.; Hayek, Y.; Naider, F.; Anglister, J. *Biochemistry* **2002**, *41*, 12687–12696.
(26) Venkatachalam, C. M. *Biopolymers* **1968**, *6*, 1425–1436.
(27) Moretto, A.; Formaggio, F.; Kaptein, B.; Broxterman, Q. B.; Wu, L.; Keiderling, T. A.; Toniolo, C. *Biopolymers* **2008**, *90*, 567–574.
(28) Toniolo, C. *CRC Crit. Rev. Biochem.* **1980**, *9*, 1–44.
(29) McPhalen, C. A.; Vincent, M. G.; Picot, D.; Jaonsonius, J. N.; Lesk, A. M.; Chothia, C. *J. Mol. Biol.* **1992**, *227*, 197–213.
(30) Gertstein, M.; Chothia, C. *J. Mol. Biol.* **1991**, *220*, 133–149.
(31) Singh, Y.; Sharpe, P. C.; Hoang, H. N.; Lucke, A. J.; McDowall, A. W.; Bottomley, S. P.; Fairlie, D. P. *Chem.—Eur. J.* **2011**, *17*, 151–160.
(32) Szőri, M.; Fittschen, C.; Csizmadia, I. G.; Viskolcz, B. *J. Chem. Theory Comput.* **2006**, *2*, 1575–1586.
(33) Sousa, S. F.; Fernandes, P. A.; Ramos, M. J. *J. Phys. Chem. A* **2007**, *111*, 10439–10452.
(34) Speck, E. J.; Olson, A.; Zhengshuang, S.; Kallenbach, N. R. *J. Am. Chem. Soc.* **1999**, *121*, 5571–5572.
(35) Becke, A. D. *Phys. Rev. A* **1988**, *38*, 3098–3100.
(36) Becke, A. D. *J. Chem. Phys.* **1996**, *104*, 1040–1046.
(37) Lee, C.; Yang, W.; Parr, R. G. *Phys. Rev. B* **1988**, *37*, 785–789.
(38) Cossi, M.; Rega, N.; Scalmani, G.; Barone, V. *J. Comput. Chem.* **2002**, *24*, 669–681.
(39) Himo, F.; Eriksson, L. A. *J. Chem. Soc., Perkin Trans. 2* **1998**, 305–308.
(40) Himo, F. *Chem. Phys. Lett.* **2000**, *328*, 270.
(41) Owen, M. C.; Komáromi, I.; Murphy, R. F.; Lovas, S. *J. Mol. Struct.* **2006**, *759*, 117–124.
(42) Szőri, M.; Abou-Abdo, T.; Fittschen, C.; Csizmadia, I. G.; Viskolcz, B. *Phys. Chem. Chem. Phys.* **2007**, *9*, 1931–1940.
(43) Shaik, S. S.; Hiberty, P. C.; Lefour, J.-M.; Ohanessian, G. *J. Am. Chem. Soc.* **1987**, *109*, 363–374.
(44) Kollmar, H. *J. Am. Chem. Soc.* **1978**, *101*, 4832–4840.
(45) Katritzky, A. R.; Soti, F. *J. Chem. Soc., Perkin Trans 1* **1974**, *1*, 1427–1432.
(46) MacInnes, I.; Walton, J. C.; Nonhebel, D. C. *J. Chem. Soc., Chem. Commun.* **1985**, 712–713.
(47) Bordwell, F. G.; Zhang, X. *J. Org. Chem.* **1990**, *55*, 6078–6079.
(48) Plusquellic, D. F.; Pratt, D. W. *J. Phys. Chem. A* **2007**, *111*, 7391–7397.
(49) Stefancic, I.; Bonifacic, M.; Asmus, K.; Armstrong, D. A. *J. Phys. Chem. A* **2001**, *105*, 8681.
(50) Galano, A.; Alvarez-Idaboy, J. R.; Montero, L. A.; Vivier-Bunge, A. *J. Comput. Chem.* **2001**, *22*, 1138–1153.
(51) Leissmann, M. H.; Hansmann, B.; Blachly, P. G.; Francisco, J. S.; Abel, B. *J. Phys. Chem. A* **2009**, *113*, 7570.
(52) Hawkins, C. L; Davies, M. J. *J. Chem. Soc., Perkin Trans.* **1998**, *2*, 2617–2622.
(53) Garrison, W. M. *Chem. Rev.* **1987**, *87*, 381–398.
(54) Vystovsky, Y. B.; Bryantsev, V. S. *Int. J. Quantum Chem.* **2004**, *96*, 123–135.
(55) Lu, H. -F.; Li, F. -Y.; Lin, S. H. *J. Comput. Chem.* **2007**, *28*, 783–794.
(56) Rauk, A.; Yu, D.; Taylor, D.; Shustov, G. V.; Block, D. A.; Armstrong, D. A. *Biochemistry* **1999**, *38*, 9089–9096.
(57) Wood, G. P. F.; Moran, D.; Jacob, R.; Radom, L. *J. Phys. Chem. A* **2005**, *109*, 6318–6325.
(58) Rauk, A. *Chem. Soc. Rev.* **2009**, *38*, 2698–2715.
(59) Allsop, D.; Mayes, J.; Moore, S.; Masad, A.; Tabner, B. J. *Biochem. Soc., Perkin Trans 1* **2008**, *36*, 1293–1298.
(60) Easton, C. J. *Chem. Rev.* **1997**, *97*, 53–82.
(61) Sperling, J.; Elad, D. *J. Am. Chem. Soc.* **1971**, *93*, 3839–3840.
(62) Elad, D.; Sinnreich, J. *J. Chem. Soc. Chem. Commun.* **1965**, 471–472.
(63) Doan, H. Q.; Davis, A. C.; Francisco, J. S. *J. Phys. Chem. A* **2010**, *114*, 5342–5357.
(64) Berkowitz, J.; Ellison, G. B.; Gutman, D. *J. Phys. Chem.* **1994**, *98*, 2744–2765.
(65) Kellogg, E. W., 3rd; Fridovich, I. *J. Biol. Chem.* **1975**, *250*, 8812–8817.
(66) Viskolcz, B.; Csizmadia, I. G.; Knack Jensen, S. J.; Perczel, A. *Chem. Phys. Lett.* **2010**, *501*, 30–32.